Cytosolic phospholipase A_2 and arachidonic acid metabolites modulate ventilator-induced permeability increases in isolated mouse lungs

Takashige Miyahara, Kazutoshi Hamanaka, David S. Weber, Mircea Anghelescu, James R. Frost, Judy A. King and James C. Parker

J Appl Physiol 104:354-362, 2008. First published 15 November 2007;
doi: 10.1152/japplphysiol.00959.2006

J Appl Physiol 104: 354–362, 2008.
First published November 15, 2007; doi:10.1152/japplphysiol.00959.2006.

Cytosolic phospholipase A_2 and arachidonic acid metabolites modulate ventilator-induced permeability increases in isolated mouse lungs

Takashige Miyahara,[1,3] Kazutoshi Hamanaka,[1,3] David S. Weber,[1] Mircea Anghelescu,[1,3] James R. Frost,[1,3] Judy A. King,[2,3] and James C. Parker[1,3]

Departments of [1]Physiology and [2]Pathology and [3]Center for Lung Biology, University of South Alabama, Mobile, Alabama

Submitted 30 August 2006; accepted in final form 9 November 2007

Miyahara T, Hamanaka K, Weber DS, Anghelescu M, Frost JR, King JA, Parker JC. Cytosolic phospholipase A_2 and arachidonic acid metabolites modulate ventilator-induced permeability increases in isolated mouse lungs. *J Appl Physiol* 104: 354–362, 2008. First published November 15, 2007; doi:10.1152/japplphysiol.00959.2006.—We previously reported that the cytosolic phospholipase A_2 ($cPLA_2$) pathway is involved in ventilator-induced lung injury (VILI) produced by high peak inflation pressures (PIP) (*J Appl Physiol* 98: 1264–1271, 2005), but the relative contributions of the various downstream products of $cPLA_2$ on the acute permeability response were not determined. Therefore, we investigated the role of $cPLA_2$ and the downstream products of arachidonic acid metabolism in the high-PIP ventilation-induced increase in vascular permeability. We perfused isolated mouse lungs and measured the capillary filtration coefficient (K_{fc}) after 30 min of ventilation with 9, 25, and 35 cmH_2O PIP. In high-PIP-ventilated lungs, K_{fc} increased significantly, 2.7-fold, after ventilation with 35 cmH_2O PIP compared with paired baseline values and low-PIP-ventilated lungs. Also, increased phosphorylation of lung $cPLA_2$ suggested enzyme activation after high-PIP ventilation. However, treatment with 40 mg/kg arachidonyl trifluoromethyl ketone (an inhibitor of $cPLA_2$) or a combination of 30 μM ibuprofen [a cyclooxygenase (COX) inhibitor], 100 μM nordihydroguaiaretic acid [a lipoxygenase (LOX) inhibitor], and 10 μM 17-octadecynoic acid (a cytochrome *P*-450 epoxygenase inhibitor) prevented the high-PIP-induced increase in K_{fc}. Combinations of the inhibitors of COX, LOX, or cytochrome *P*-450 epoxygenase did not prevent significant increases in K_{fc}, even though bronchoalveolar lavage levels of the COX or LOX products were significantly reduced. These results suggest that multiple mediators from each pathway contribute to the acute ventilator-induced permeability increase in isolated mouse lungs by mutual potentiation.

capillary permeability; ventilator-induced lung injury; cyclooxygenase; lipoxygenase; leukotrienes; cytochrome *P*-450

THE ACUTE RESPIRATORY DISTRESS syndrome (ARDS) network study has demonstrated the importance of a reduced tidal volume in preventing ventilator-induced lung injury (VILI) produced by high peak inflation pressures (PIP) and tidal volumes (7). Elevated levels of cytosolic phospholipase A_2 ($cPLA_2$), leukotrienes (LTs), and cyclooxygenase (COX) products have been reported in bronchoalveolar lavage fluid (BALF) from ARDS patients (11, 26). In animal models, microvascular permeability is acutely increased after only 20 min of high-PIP ventilation, whereas proinflammatory cytokine production was delayed and variable (36, 45). Inhibition of $cPLA_2$ with arachidonyl trifluoromethyl ketone (ATK) prevented VILI in Clara cell secretory protein-knockout and wild-type mice (46) and in mice with endotoxin-induced lung injury (24). These results support the concept of a rapid onset of increased capillary permeability in response to lung overdistension mediated by rapid signal transduction through the $cPLA_2$ pathways. Protein leak and edema may then contribute to release of cytokines and propagation of inflammation that further increase lung injury (31, 45, 46).

Activated $cPLA_2$ can have myriad proinflammatory effects by catalyzing the hydrolysis of phospholipids to lysophospholipids (17), platelet-activating factor (PAF) (13), and arachidonic acid (AA) (3). AA is further metabolized by cyclooxygenase (COX), lipoxygenase (LOX), and cytochrome *P*-450 epoxygenase (*P*-450) pathways to inflammatory mediators such as prostaglandins (PG), thromboxanes (TXs), LTs, and epoxyeicosatrienoic acids (EETs) (47). Inhibition of $cPLA_2$ may attenuate VILI by reducing these numerous downstream products, which can increase vascular permeability, recruit neutrophils, and injure cells (23). We recently identified the transient receptor potential vanilloid-4 (TRPV4) channel as the stretch-activated cation channel that initiates VILI (15). These channels are activated by PLA_2-derived AA and its *P*-450 derivatives. However, the relative contributions of the specific downstream products of AA to the rapid initial permeability increase in high-PIP injury remain to be identified.

In the present study, we used specific inhibitors of $cPLA_2$ activity and the activities of each of the major downstream enzymatic pathways of AA metabolism to investigate the contributions of $cPLA_2$ activity and the endogenously produced downstream products of AA metabolism to the acute vascular permeability response to high-PIP ventilation in isolated perfused mouse lungs. Acute changes in vascular permeability were evaluated using the capillary filtration coefficient (K_{fc}), a sensitive index of capillary hydraulic conductivity, as well as BALF albumin concentration, lung wet-to-dry weight ratios (W/D), and histological examination. Our data demonstrate that $cPLA_2$ inhibition significantly attenuated the increase in K_{fc} after high-pressure ventilation, but only a combination of all pathway inhibitors significantly attenuated the increased permeability. These findings suggest that multiple downstream products regulated by the $cPLA_2$ pathway modulate the VILI-induced increase in acute microvascular permeability.

MATERIALS AND METHODS

All experimental protocols were approved by the Institutional Animal Care and Use Committee of the University of South Alabama

Address for reprint requests and other correspondence: J. C. Parker, Dept. of Physiology, MSB 3074, College of Medicine, Univ. of South Alabama, Mobile, AL 36688 (e-mail: jparker@usouthal.edu).

The costs of publication of this article were defrayed in part by the payment of page charges. The article must therefore be hereby marked "*advertisement*" in accordance with 18 U.S.C. Section 1734 solely to indicate this fact.

College of Medicine. Anesthetized mice were killed by exsanguination at the time of heart and lung removal.

Isolated lung preparations. C57BL/6 male mice [n = 65, 17.5–26.6 (23.3 ± 0.23) g; Jackson Laboratory] were anesthetized with pentobarbital sodium (100 mg/kg ip). The trachea was cannulated, and the lungs were ventilated with 20% O_2-5% CO_2-75% N_2 by a rodent ventilator (model 683, Harvard, South Natick, MA). The tidal volume was adjusted to obtain ~9 cmH_2O PIP at a respiratory rate (RR) of 40 breaths/min. The chest was opened, heparin (100 IU) was injected into the left ventricle, and a suture was placed around the pulmonary artery and aorta. Cannulas (0.86 mm ID, 1.27 mm OD) were placed in the pulmonary artery and left atrium, and the lungs and heart were removed en bloc and suspended from a balance beam attached to a force transducer (model FT03C, Grass, Quincy, MA). Plastic drapes around the preparation eliminated weight artifacts caused by air currents. The initial 1–2 ml of perfusate, which contained residual blood cells and plasma, were discarded and not recirculated. To exclude binding of each inhibitor to proteins in the perfusate, all lungs were perfused with 1% BSA-3% clinical-grade dextran 70 in Krebs bicarbonate buffer (2) via a roller pump (Minipuls2, Gilson, Middleton, WI) at a constant flow rate of 0.75 ml/min in a recirculating system with a system volume of 10 ml. Temperature was maintained at 37°C by a heating tape. The venous outflow was collected in a reservoir, the height of which could be adjusted to increase venous pressure. Pulmonary arterial (P_{pa}), pulmonary venous (P_{pv}), and airway pressures were measured with a pressure transducer (Cobe, Lakewood, CO) that was zeroed at the midlung level, and pressures and lung weight were recorded on a polygraph (model 7D, Grass).

Pulmonary vascular resistances. Total resistance (R_t) and segmental pulmonary vascular resistance were calculated from the perfusate flow and the differences between P_{pa}, P_{pv}, and double-occlusion capillary pressure (P_{pc}) as follows: $R_t = (P_{pa} - P_{pv})/(\dot{Q}/100\ g)$, precapillary resistance (R_a) = $(P_{pa} - P_{pc})/(\dot{Q}/100\ g)$, and postcapillary resistance (R_v) = $(P_{pc} - P_{pv})/(\dot{Q}/100\ g)$, where $\dot{Q}$ is perfusate flow. All resistance was normalized to predicted lung weight (i.e., $cmH_2O \cdot l^{-1} \cdot min \cdot 100\ g^{-1}$).

K_{fc}. K_{fc} ($ml \cdot min^{-1} \cdot cmH_2O^{-1} \cdot 100\ g^{-1}$) is a sensitive measurement of endothelial hydraulic conductivity in fully recruited lungs (33). After an isogravimetric state is attained, P_{pv} was increased by 6 cmH_2O for 20 min (Fig. 1), and the change in capillary pressure was determined by double occlusion before and after the P_{pv} increase. K_{fc} was calculated as the rate of lung weight gain between 18 and 20 min divided by the change in P_{pc}. All K_{fc} values were normalized to 100 g predicted lung weight on the basis of the ratio of lung weight to body weight (BW) according to predicted lung weight (PLW) as follows: PLW = (0.00452 ± 0.0003)BW (30).

Isolated lung protocols. The time course for venous pressure and PIP of the high- and low-PIP-ventilation groups are shown in Fig. 1. In all experiments, the lungs were perfused and ventilated for 30 min in an isogravimetric state with 9 cmH_2O PIP and 2.5 cmH_2O positive end-expiratory pressure (PEEP) at an RR of 40 breaths/min, and then vascular occlusion pressure and K_{fc} were measured. Subsequently, lungs were perfused and ventilated for 30 min with 25 and 35 cmH_2O PIP and 2.5 cmH_2O PEEP. Although tidal volumes were not measured, estimates of tidal volume at 9, 25, and 35 cmH_2O PIP are 0.45, 1.23, and 1.73 ml, respectively, on the basis of lung compliance estimates for C57BL/6 mice (39). At 30 and 80 min after the initial K_{fc} measurement, occlusion pressure and K_{fc} for 20 min were repeated for a total of three K_{fc} measurements.

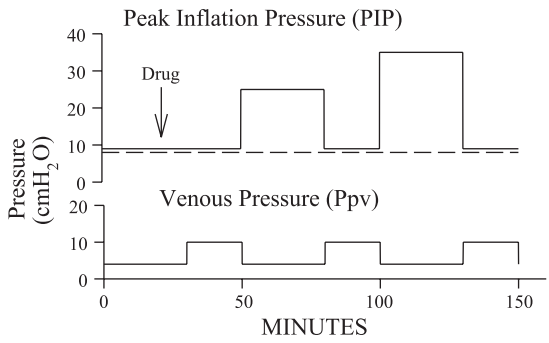

Fig. 1. Time course of venous pressure (P_{pv}, *bottom solid line*) increases for capillary filtration coefficient (K_{fc}) measurements and peak inflation pressure (PIP) increases during ventilation periods in all groups subjected to high-PIP ventilation (*top solid line*) or low-PIP ventilation (*top dashed line*).

Treatment groups. The lungs were randomly allocated to one of the following 10 groups.

Group 1 (low-PIP control group, n = 6) was ventilated with 9 cmH_2O PIP and 2.5 cmH_2O PEEP throughout the experiments. *Group 2* (high-PIP injury group, n = 10) was ventilated with the high-PIP protocol only. *Group 3* (ATK group, n = 9) was ventilated with the high-PIP protocol after pretreatment 30 min before the first K_{fc} measurement with ATK (40 mg/kg body wt), an inhibitor of cPLA$_2$ (46). *Group 4* (COX group, n = 4) was ventilated with the high-PIP protocol after pretreatment with 30 μM ibuprofen, a COX inhibitor (2). *Group 5* (LOX group, n = 4) was ventilated with the high-PIP protocol after pretreatment with 100 μM nordihydroguaiaretic acid, an LOX inhibitor (22). *Group 6* (*P*-450 group, n = 4) was ventilated with the high-PIP protocol after pretreatment with 10 μM 17-octadecynoic acid, a *P*-450 inhibitor (2).

Some lungs were treated with a combination of two or three inhibitors as follows. *Group 7* (COX + LOX group, n = 6) was ventilated with the high-PIP protocol after pretreatment with the COX and LOX inhibitors described above. *Group 8* (LOX + *P*-450 group, n = 6) was ventilated with the high-PIP protocol after pretreatment with the LOX and *P*-450 inhibitors described above. *Group 9* (COX + *P*-450 group, n = 6) was ventilated with the high-PIP protocol after pretreatment with the COX and *P*-450 inhibitors described above. *Group 10* (COX + LOX + *P*-450 group, n = 10) was ventilated with the high-PIP protocol after pretreatment with all three inhibitors for COX, LOX, and *P*-450 described above. These inhibitors were added to the perfusate 30 min before PIP ventilation for 30 min at 25 cmH_2O.

BALF protein and AA metabolites. The right lung was lavaged four times with 0.5 ml of PBS. Albumin concentrations were measured with an ELISA (Bethyl, Montgomery, TX). Concentrations of 6-keto-$PGF_{1\alpha}$, the stable metabolite of PGI_2, and the cysteinyl LTs (LTC_4, LTD_4, and LTE_4) were also measured using ELISA kits (Cayman Chemical, Ann Arbor, MI).

W/D. At the end of the experiments, the left lung was tied at the left hilum and then removed. The wet weight of the left lung was recorded, and the lung was desiccated at 80°C for 1 wk before dry weight was measured for W/D.

Western analysis for phosphorylated cPLA$_2$. For protein extraction, tissue samples were minced and sonicated, cells were lysed in ice-cold buffer (in mM: 50 HEPES, 5 EDTA, 100 NaCl) at 4°C for 1 h (pH 7.4), 1% Triton X-100, protease inhibitors (10 μg/ml aprotinin, 1 mM phenylmethylsulfonyl fluoride, and 10 μg/ml leupeptin), and phosphatase inhibitors (in mM: 50 sodium fluoride, 1 sodium orthovanadate, 10 sodium pyrophosphate, and 0.001 microcystin). Solubilized proteins were isolated by centrifugation at 27,000 *g* for 15 min, and protein concentrations of the supernatant were determined using the Bradford assay. For Western analysis, samples were boiled in 1× SDS buffer, separated using SDS-PAGE, and subsequently transferred to nitrocellulose membranes. Membranes were blocked at room temperature for 1 h in TBS containing 5% milk and 0.1% Tween 20. Lung homogenates were also separated into membrane-bound (hydrophobic) and cytosolic (hydrophilic) proteins with use of a Mem-PER protein extraction kit (Pierce Biotechnology, Rockford, IL) and probed for phosphorylated cPLA$_2$. Primary antibodies to phosphorylated (Ser^{505}) cPLA$_2$ and total cPLA$_2$ were obtained from Cell Signaling (Danvers, MA). After incubation with primary and second-

ary antibodies, proteins were detected by enhanced chemiluminescence, and band intensities were quantified using Sigmagel software.

Histology. A portion of the right lung was ligated and sectioned for histological examination. Sections were fixed in 10% buffered formalin, embedded in paraffin, cut with a microtome to 5 μm thickness, and stained with hematoxylin and eosin. Slides were viewed by a blinded referee using light microscopy for histological evaluation of injury. Light microscopy in glutaraldehyde-fixed lungs was used to evaluate quantitative edema distribution in perivascular cuffs. In 1-μm-thick sections, extra-alveolar vessel cuff volume (V_c) fraction of total wall volume (V_c/V_w) was determined using a point-counting strategy (1). Point-counting analysis was performed in four experiments in each of the low-PIP control, high-PIP injury, and ATK groups and three experiments in the COX + LOX + *P*-450 group. Means for vessel diameter and volume fractions were determined for each lung, and overall descriptive statistics were derived for each group.

Statistical analysis. Values are means ± SE. A one- or two-way ANOVA with repeated measures followed by Student-Newman-Keuls or Fisher's least significant difference post hoc test was used as indicated for comparison of groups. Significant differences were determined by $P < 0.05$.

RESULTS

Microvascular permeability. Figure 2 shows the effects of each inhibitor combination on K_{fc} in isolated perfused lungs. In the high-PIP injury group, K_{fc} increased significantly, 2.7-fold, from baseline after high-PIP ventilation 80 min after baseline K_{fc}, but K_{fc} was not significantly increased 30 min after baseline K_{fc}. K_{fc} was also significantly higher in the high-PIP injury group than in the low-PIP control, ATK, and COX + LOX + *P*-450 groups. Pretreatment with ATK significantly attenuated the increase in the final K_{fc} compared with the high-PIP injury group, although K_{fc} in the ATK group was significantly higher than baseline K_{fc}. This indicates that ATK did not completely prevent the increase in permeability induced by high-PIP ventilation. Also, the final K_{fc} of all except the low-PIP control group was significantly increased compared with paired baseline K_{fc} values. Use of a single inhibitor in the COX, LOX, or *P*-450 experiments or a combination of two inhibitors in the COX + LOX, COX + *P*-450, or LOX + *P*-450 experiments did not significantly attenuate the K_{fc} increase compared with the untreated high-PIP injury group. Only the combination of all three inhibitors in the COX + LOX + *P*-450 group significantly attenuated the high-PIP-induced increase in permeability to the same degree observed in the ATK group. Relative to the high-PIP injury group, the final K_{fc} values were 30% for the low-PIP control group, 46% for the ATK group, and 49% for the COX + LOX + *P*-450 group.

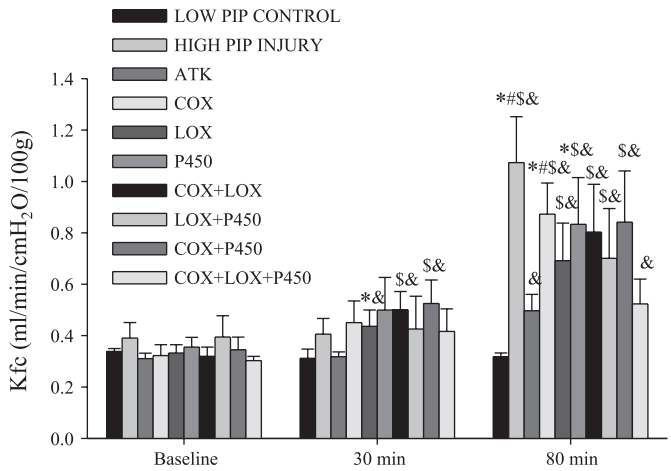

Fig. 2. K_{fc} as a function of time. K_{fc} increased 2.7-fold (from baseline of 0.391 ± 0.061 to 1.074 ± 0.178 ml·min^{-1}·cmH_2O^{-1}·100 g^{-1}) after 35 cmH_2O PIP with 2.5 cmH_2O positive end-expiratory pressure (PEEP) at 100 min in high-PIP injury group. Increase in K_{fc} was significantly attenuated in the group pretreated with arachidonyl trifluoromethyl ketone (ATK) inhibitor, and combination of cyclooxgenase (COX), lipoxygenase (LOX), and cytochrome P-450 epoxygenase (*P*-450) inhibitor prevented an increase in permeability. Values are means ± SE. *$P < 0.05$ vs. ATK group; #$P < 0.05$ vs. COX + LOX + *P*-450 group; \$$P < 0.05$ vs. low-PIP control group in the same time period. &$P < 0.05$ vs. baseline in the same group.

Table 1 summarizes lung W/D and albumin concentrations in BALF. Since W/D was dependent on vascular pressure and time of filtration, as well as K_{fc}, these variables proved less sensitive than K_{fc} to differences in permeability. Although W/D was significantly greater in all groups, except the ATK group, than in the low-PIP control group, W/D in the high-PIP injury and COX + LOX + *P*-450 groups was not significantly different from W/D in the ATK group. However, W/D of the ATK group was not significantly different from that of the low-PIP control group. Relative to the high-PIP injury group, final W/D was 80% for the low-PIP control group, 93% for the ATK group, and 94% for the COX + LOX + *P*-450 group. BALF albumin concentration was significantly lower (34%) in the ATK group than in the high-PIP injury group and significantly lower than in all other groups, except the low-PIP control group. BALF albumin was also significantly lower (19%) in the COX + LOX + *P*-450 group than in the high-PIP injury group. There was also a significant difference between the COX + LOX + *P*-450 group and the LOX, COX + LOX, and COX + *P*-450 groups. Relative to the high-PIP injury group, the final BALF albumin concentrations were 48% for the low-PIP control group, 50% for the ATK group, and 62% for the COX + LOX + *P*-450 group. Taken together, these measurements demonstrated that ATK and the combination of COX, LOX, and *P*-450 inhibitors significantly attenuated the increased permeability induced by high-PIP ventilation.

Pulmonary hemodynamics. Pulmonary hemodynamics of all groups are shown in Table 2. There were no differences in baseline hemodynamics between groups. Ventilation and measurement of K_{fc} resulted in a small decrease in R_t in all groups at 50 min. R_t, and especially R_v, decreased significantly at the end of experiment in the low-PIP control group. Resistance of the other groups tended to increase from baseline values at the end of the experiments.

Phosphorylation of cPLA$_2$. Western blots of lung tissue homogenates demonstrated a significant, 2.2-fold, increase in phosphorylated cPLA$_2$ after high-PIP ventilation compared with low-PIP ventilation (Fig. 3*A*). The total cPLA$_2$ was not significantly different between groups. Separation of the homogenates into cytosol and membrane components indicated a significant, 1.8-fold, increase in membrane-associated phosphorylated cPLA$_2$ and a trend toward an increase in phosphorylated cPLA$_2$ in the high-PIP ventilation group (Fig. 3*B*).

BALF AA metabolites. AA metabolites in BALF were determined using an ELISA (Fig. 4). Lavage concentrations of 6-keto-PGF$_{1\alpha}$ were significantly lower in all groups, except the LOX + *P*-450 group, than in the high-PIP injury group (Fig. 3*A*). Lavage concentrations of the cysteinyl LTs were signifi-

Table 1. *Terminal lung wet-to-dry weight ratios and BALF albumin concentrations*

Group	W/D	BALF Albumin, mg/ml
Low-PIP control	6.31±0.39	48.24±1.82
High-PIP	7.84±0.20†	76.12±3.73*†‡
ATK	7.28±0.26	50.14±1.14
COX	7.48±0.73†	68.93±2.33*†
LOX	7.55±0.42†	74.15±2.83*†‡
P-450	7.87±0.59†	64.61±4.62*†
COX + LOX	7.40±0.33†	71.18±1.30*†‡
LOX + *P*-450	7.80±0.33†	58.81±5.83*†
COX + *P*-450	7.98±0.41†	72.47±5.20*†‡
COX + LOX + *P*-450	7.39±0.28†	61.58±2.09*†

Values are means ± SE. W/D, lung wet-to-dry weight ratio; BALF, bronchoalveolar lavage fluid; PIP, peak inflation pressure; ATK, arachidonyl trifluoromethyl ketone; COX, cyclooxygenase; LOX, lipoxygenase; *P*-450, cytochrome *P*-450 epoxygenase. *$P < 0.05$ vs. ATK. †$P < 0.05$ vs. low-PIP control. ‡$P < 0.05$ vs. COX + LOX + *P*-450.

cantly lower in all groups, except the COX and COX + *P*-450 groups, than in the high-PIP injury group (Fig. 3*B*). Thus COX and LOX pathway products were significantly increased by high-PIP ventilation compared with low-PIP ventilation for the same periods. As expected, mean values of the COX or LOX pathway products tended to be lower in the groups treated with the COX or LOX inhibitors.

Histological findings. Microscopic examinations were performed on all groups, but only micrographs from the low-PIP control, high-PIP injury, ATK, and COX + LOX + *P*-450 groups are shown in Fig. 5*A*. Sloughing of epithelial cells was not observed in any group. Since all lungs were perfused with buffer, no differences in inflammatory cell numbers were observed. The major feature shown by light microscopy was perivascular edema cuffs, primarily around arteries and, to a lesser extent, around veins. Perivascular edema cuffs were large and prevalent in the high-PIP injury group but small and infrequent in the low-PIP control group, but more regions of atelectasis were observed in the low-PIP control group than the other groups. The cuff sizes were generally smaller and less frequent in the ATK and COX + LOX + *P*-450 groups than in the groups treated with one or two of the inhibitors. Figure 5*B* shows a morphometric analysis of V_c/V_w for four groups. Point-counting analysis was performed for four experiments in each of the low-PIP control, high-PIP injury, and ATK groups and three experiments in the COX + LOX + *P*-450 group. The number of cuffs, mean vessel diameter, and maximum and minimum diameters were $n = 49$, 59 ± 6 μm, and 158–25 μm for the low-PIP control group; $n = 55$, 57 ± 4 μm, and 137–25 μm for the high-PIP injury group; $n = 17$, 72 ± 9 μm, and 163–25 μm for the COX + LOX + *P*-450 group; and $n = 47$, 60 ± 5 μm, and 167–25 μm for the low-PIP control group. V_c/V_w was significantly greater for the high-PIP injury (3.3-fold), ATK (2.2-fold), and COX + LOX + *P*-450 (2.1-fold) groups than for the low-PIP control group. V_c/V_w was also significantly higher for the high-PIP injury group than for the ATK group.

DISCUSSION

In the present study, we determined the role of cPLA$_2$ and the downstream products of AA metabolism in the increases in permeability induced by acute high-PIP ventilation in isolated mouse lungs. We previously reported that ATK, an inhibitor of cPLA$_2$, attenuated the VILI-induced increase in permeability in intact mouse lungs (46). The increase in vascular permeability due to high-volume ventilation appears rapidly, before significant increases in cytokines (36, 45). The major new findings of the present study are as follows. *1*) cPLA$_2$ inhibition also significantly attenuated the high-PIP-induced increase in vascular permeability in isolated mouse lungs. *2*) Permeability was not prevented by blockade of only one or two of these downstream pathways, but a combination of inhibitors simultaneously targeting all three downstream pathways of AA metabolism attenuated the increase in permeability and edema formation by approximately the same amount as inhibition of cPLA$_2$. These findings suggest that cPLA$_2$ plays a crucial role in the pathogenesis of acute VILI and that multiple downstream products of AA have mutually potentiating effects to produce this increase in permeability.

Isolated lung preparations have become a standard tool for measuring rapid increases in lung vascular permeability. K_{fc} is a measure of endothelial hydraulic conductivity independent of filtration pressure, because filtration rate is normalized to microvascular pressure and lung weight (surface area) (5, 30, 33). Since W/D and, to some extent, the convective transport of albumin into the alveoli are dependent on the filtration pressure and the time for filtration (33, 40), K_{fc} is a more sensitive indicator of endothelial barrier properties. In addition, filtration and K_{fc} change as transcapillary pore radius to the fourth power, whereas BALF albumin fluxes vary as the pore radius

Table 2. *Pulmonary vascular resistance*

	R_t			R_a			R_v		
Group	Baseline	50 min	100 min	Baseline	50 min	100 min	Baseline	50 min	100 min
Low-PIP control	16.49±0.89	14.26±0.72	13.09±0.56*	8.86±0.78	7.87±0.63	7.18±0.61	7.63±0.32	6.39±0.28	5.91±0.19*
High-PIP	16.06±1.12	14.30±0.84	16.67±0.92†	9.08±0.96	8.26±0.53	9.75±0.66	6.98±0.21	6.04±0.46	6.92±0.38
ATK	16.15±0.44	14.64±0.60	16.34±0.47†	8.87±0.43	7.56±0.33	8.88±036	7.28±0.48	7.80±0.54	7.45±0.38†
COX	16.04±1.21	15.85±1.25	18.04±1.28†	8.33±0.83	8.24±0.61	10.14±1.04	7.71±1.15	7.62±0.91	7.90±0.81†
LOX	16.11±1.49	14.89±1.39	17.37±0.65†	9.02±0.89	8.23±0.26	9.80±0.30	7.09±0.62	6.66±1.14	7.57±0.45†
P-450	15.55±0.41	14.13±0.93	16.31±0.59	8.81±0.20	8.07±0.50	9.84±0.20	6.73±0.30	6.06±0.42	6.47±0.55
COX+LOX	15.54±1.00	14.75±0.93	16.54±1.39	9.08±0.72	8.76±0.65	10.10±0.86	6.46±0.43	5.98±0.30	6.44±0.57
LOX+*P*-450	15.21±0.59	14.27±0.67	16.56±1.17	8.83±0.43	8.12±0.49	9.42±0.63	6.38±0.27	6.15±0.26	7.14±0.59
COX+*P*-450	15.41±0.83	14.77±1.00	17.12±1.46	9.25±0.64	8.65±0.61	10.57±0.91	6.16±0.30	6.11±0.41	6.55±0.60
COX+LOX+*P*-450	16.21±0.57	15.34±0.26	16.43±0.60	9.66±0.53	8.85±0.25	9.57±0.43	6.55±0.20	6.48±0.13	6.85±0.31

Values are means ± SE, expressed in $cmH_2O \cdot l^{-1} \cdot min \cdot 100\ g^{-1}$. R_t, total pulmonary vascular resistance; R_a, pulmonary arterial resistance; R_v, pulmonary venous resistance. *$P < 0.05$ vs. baseline within the same group. †$P < 0.05$ vs. low-PIP control in the same time period.

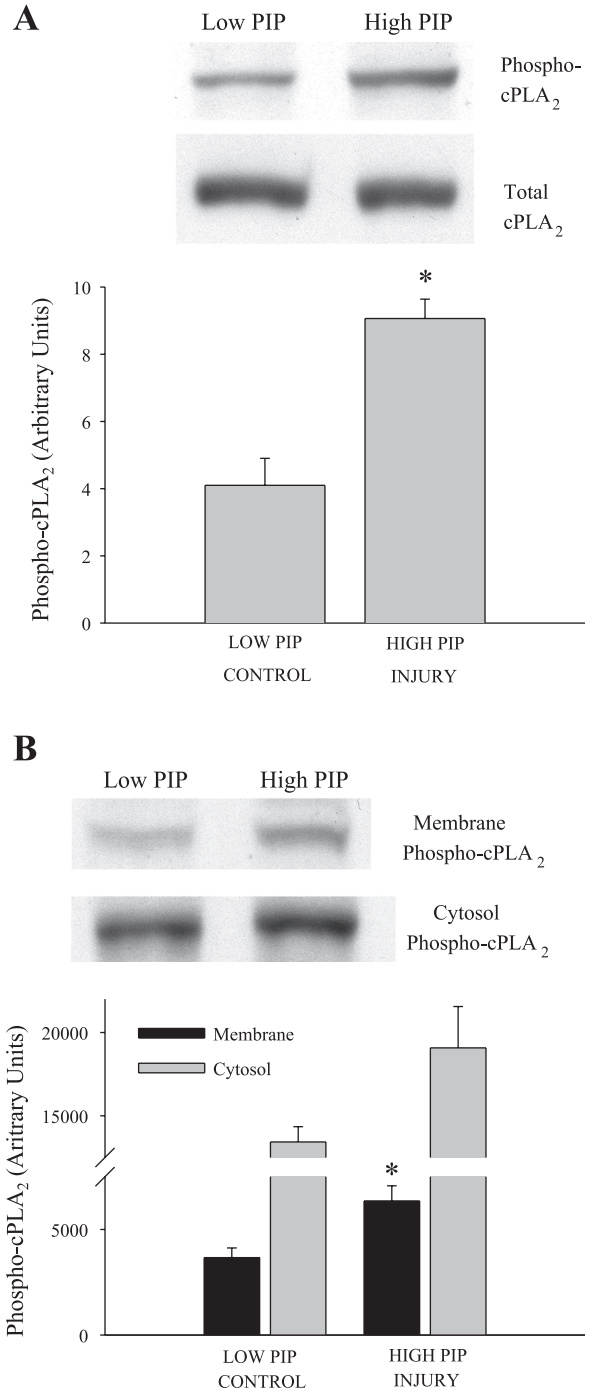

Fig. 3. Representative Western blots of phosphorylated cytosolic phospholipase A$_2$ (cPLA$_2$) in lung tissue homogenates in low-PIP control and high-PIP injury groups. *A*: total and phosphorylated cPLA$_2$ in lung tissue homogenates. *B*: phosphorylated cPLA$_2$ in membrane and cytosol fractions of lung tissue homogenates. *$P < 0.05$ vs. low-PIP control group.

squared (9, 40). Using K_{fc} measurements, we could discriminate relatively modest increases in vascular permeability. The magnitudes of the differences between high- and low-PIP ventilation and the effect of inhibitors were much greater for K_{fc} measurements than BALF albumin concentrations or W/D (see RESULTS). In contrast to BALF albumin concentrations or W/D, K_{fc} measurements are independent of time and vascular pressure effects. This resulted in a better statistical resolution of differences between the high-PIP injury group and the injury-inhibitory effects in the low-PIP control, ATK, and COX + LOX + *P*-450 groups. K_{fc} measurements indicated that the ATK and COX + LOX + *P*-450 groups significantly protected against the increased permeability of high-PIP ventilation, even though these K_{fc} values were significantly higher than K_{fc} of the low-PIP group. BALF albumin was also significantly lower in the ATK and COX + LOX + *P*-450 groups than in the high-PIP group but significantly lower in the ATK group than in the COX + LOX + *P*-450 group. W/D values were statistically significantly different in the high- and low-PIP groups, but W/D values in the ATK group were not statistically greater than those in the low-PIP group. However, morphometric estimates of cuff volumes did indicate statistically significantly smaller volumes in the ATK and COX + LOX + *P*-450 groups than in the high-PIP group. Since we assessed lung injury using W/D and BALF albumin and protein concentration in our previous study of cPLA$_2$ inhibition in intact mice (46), we sought to confirm our previous observation that inhibition of cPLA$_2$ could inhibit the increased permeability induced by VILI by measuring K_{fc} in isolated mouse lungs (46).

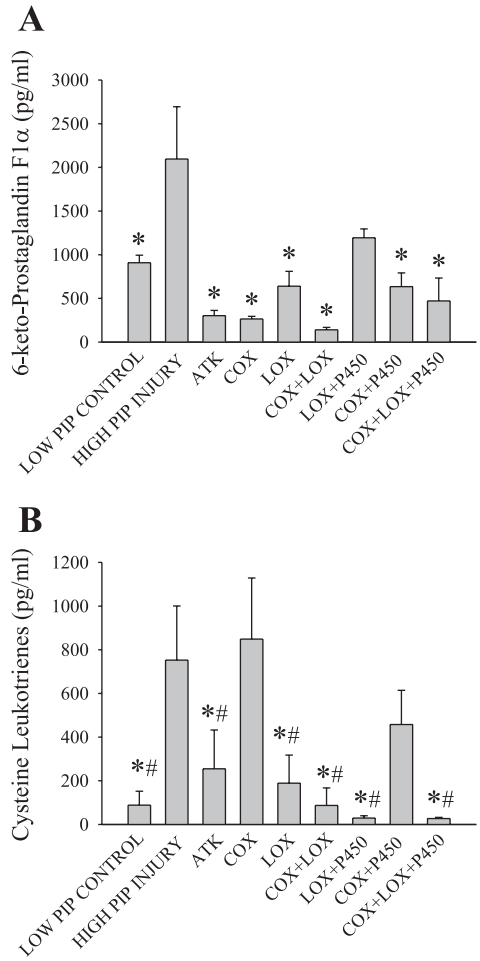

Fig. 4. Arachidonic acid metabolites in bronchoalveolar lavage fluid from all groups determined using an ELISA for 6-keto-PGF$_{1\alpha}$ (*A*) and cysteinyl leukotrienes (*B*). *$P < 0.05$ vs. high-PIP injury group. #$P < 0.05$ vs. COX group.

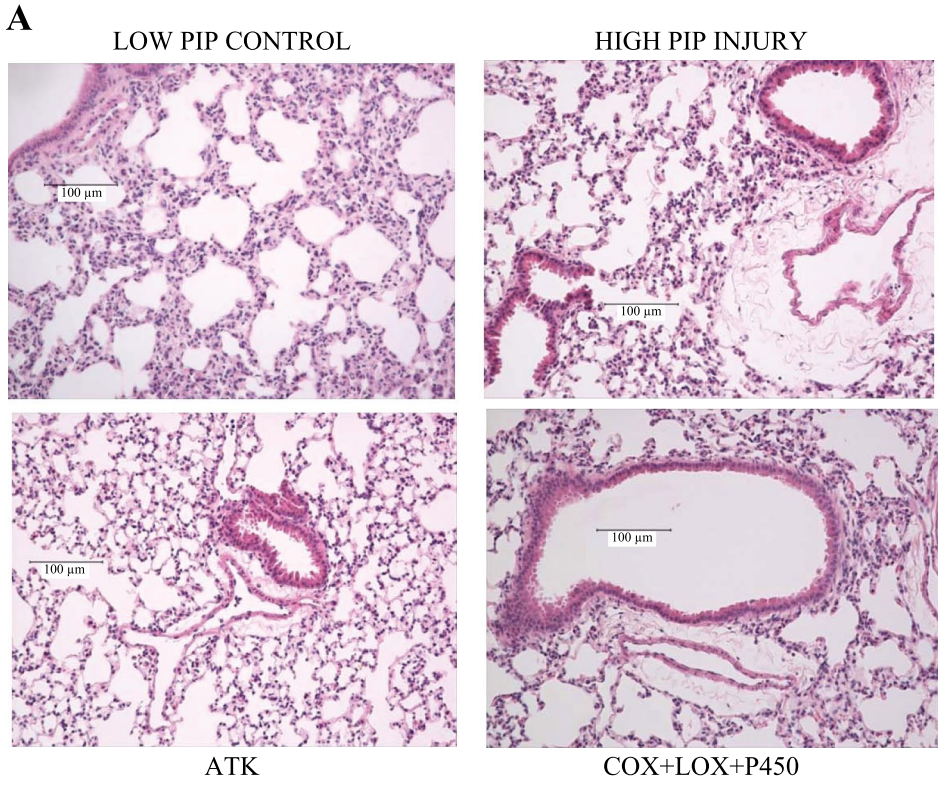

Fig. 5. *A*: lung tissue from low-PIP control, high-PIP injury, ATK, and COX + LOX + *P*-450 groups. Sections were stained with hematoxylin and eosin. *B*: ratio of edema cuff volume to total vascular wall volume (V_c/V_w) of vessels in low-PIP control, high-PIP injury, ATK, and COX + LOX + *P*-450 groups. *$P <$ 0.05 vs. low-PIP group. #$P < 0.05$ vs. ATK group.

cPLA$_2$ is an 85-kDa protein that is widely distributed in cells and is activated by submicromolar intracellular Ca^{2+} concentrations and phosphorylation by activated MAPK during high-PIP ventilation (20, 47). Phosphorylated cPLA$_2$ then moves to the cell membrane to liberate AA (23). Ca^{2+} and MAPK activation increase in stretched endothelial cell monolayers as well as in in situ endothelial and epithelial cells in intact lungs during overdistension (4, 27). PLA$_2$ activation has also been reported in endothelial cells in culture (35) and in intact blood-perfused lungs after mechanical stress (19). In the present study, cPLA$_2$ phosphorylation was increased by high-PIP ventilation compared with low-PIP ventilation in mouse lungs, which, together with the increases in downstream COX and LOX, indicates activation of cPLA$_2$ by high-PIP ventilation. A second type of PLA$_2$, the lower-molecular-weight secretory phospholipase A$_2$ (sPLA$_2$), is normally present in some lung cell types, but a spontaneous disruption of the sPLA$_2$ gene in exon 3 in inbred strains of C57BL/6 mice (18) precludes its contribution to the PLA$_2$ activity in the present studies. A third type, the Ca^{2+}-independent form of PLA$_2$ (iPLA$_2$) is primarily a housekeeping enzyme for specialized phospholipids; in the mouse, it is present primarily in the digestive tract and only in trace amounts in the lung (23). A fourth group of proteins with PLA$_2$ activity are the PAF acetyl hydrolases, which have substrate specificity for PAF but do not appear to be involved in AA release (6). Although the ATK dose used in the present study also inhibits iPLA$_2$, the contribution of iPLA$_2$ to the lung responses described here is likely to be small. ATK may also have some inhibitory effects on the COX pathway, but since this pathway is downstream of PLA$_2$, the primary effect of ATK in the present study is considered to be on cPLA$_2$ (6). The major downstream routes of AA metabolism include oxygenation by COX, LOX, or *P*-450 monooxygenases (6).

Isolated lung studies and endothelial and epithelial monolayer experiments provide putative evidence that VILI is initiated by mechanogated Ca^{2+} entry through nonselective cation channels (28). Parker et al. (31, 34) reported that high-PIP-induced increases in filtration coefficients were attenuated using gadolinium chloride, a stretch-activated cation channel and nonspecific Ca^{2+} channel blocker. Recent evidence indicates that the mechanogated channel that initiates the increased vascular permeability of VILI is the TRPV4 channel protein (15, 38). These channels were activated by mechanical stress and secondarily by mechanical stimulation of PLA_2 activity and subsequent AA release (43). *P*-450 derivatives of AA metabolism, in particular 5,6-EET, strongly activate the TRPV4 channels (44). Alvarez et al. (1, 2) reported that infusion of 5,6- and 14,15-EET increased K_{fc} in isolated mouse and rat lungs, and this increase was blocked by ruthenium red, a TRP channel inhibitor. Recently, Hamanaka et al. (15) observed that the high-PIP-induced permeability increases in isolated mouse lungs were blocked by the TRPV channel inhibitor ruthenium red, methanandamide, an inhibitor of AA production, and miconazole, a *P*-450 inhibitor, and was absent in lungs from TRPV4-knockout mice. Thus metabolites of the *P*-450 pathway are major contributors to the increased vascular permeability induced by VILI, apparently by facilitating Ca^{2+} entry through stretch-activated cation channels.

Measurement of the stable product of PGI_2 degradation, 6-keto-$PGF_{1\alpha}$, and the cysteinyl LTs indicates that high-PIP ventilation significantly increased COX and LOX products in lavage fluid compared with low-PIP ventilation. Blockade of PLA_2 during high-PIP ventilation attenuated the products of COX and LOX pathways and significantly attenuated the K_{fc} increase. Although inhibition of the COX or LOX pathways alone preferentially reduced the products of the inhibited pathway, separate pathway inhibition was less effective in reducing the K_{fc} increase after high-PIP ventilation. The inhibitory responses in these studies and previous studies indicate that the doses of inhibitors were sufficient to block the target pathways. Nagase et al. (24) found that pretreatment with only 20 mg/kg of the slow-binding, but effective, PLA_2 inhibitor ATK was sufficient to significantly reduce BALF LTB_4, TXB_2, and the cysteinyl LTs LTC_4, LTD_4, and LTE_4 in a mouse model of LPS-zymosan lung injury. Similarly, the dose of 17-octadecynoic acid would be expected to effectively inhibit *P*-450, because its IC_{50} values for inhibition of ω-hydroxylation and epoxidation were 7 and 5 μM, respectively (42). Effective doses of ibuprofen and nordihydroguaiaretic acid, the nonselective inhibitors of the COX and LOX pathways, were also used.

Lipid mediators are known to play a significant role in lung endothelial and alveolar epithelial barrier function (24, 25). We hypothesized that many of the endogenous levels of the downstream products of AA metabolism have the potential to increase vascular permeability. Release of PGE_2, PGI_2, and TXA_2 is edemagenic during acute lung inflammation, as is release of nonenzymatically produced prostanes (29). Release of TXB_2, the stable product of TXA_2, was significantly greater in the perfusate in isolated rabbit lungs after high-PIP ventilation than after low-PIP ventilation (12). On the other hand, there were no detectable levels of TX, LTB_4, and PGE_2 and no change in COX-2 mRNA expression in the perfusate in isolated mouse lung with negative- or positive-pressure hyperventilation (41). The present study demonstrated that inhibition of all three major pathways in the COX + LOX + *P*-450 group, but not inhibition of only two pathways in the LOX + *P*-450 group, attenuated the increase in permeability. This finding suggests that the COX pathway might contribute to VILI-induced increases in permeability, but the COX inhibitor alone did not attenuate the increase in permeability, even though 6-keto-$PGF_{1\alpha}$ was significantly decreased in lavage fluid in all COX inhibitor-treated groups. Thus inhibition of mediators derived from a single pathway had no effect on the magnitude of the increased permeability, even though many of these mediators infused in very high concentrations have the potential to increase vascular permeability. Potentiation of effects of multiple mediators may occur through activation of multiple second messenger pathways, which together initiate the permeability response (16). Another mechanism may be competition for AA substrate between the various AA pathways. For example, in the presence of COX blockade, as in the COX group, AA metabolites appear to be shifted toward the LOX and *P*-450 pathways (10).

Studies of patients with ARDS indicated markedly elevated levels of LTs in pulmonary edema fluid compared with edema fluid from patients with hydrostatic pulmonary edema (21). LTB_4, a potent neutrophil chemoattractant, appears to have a significant role in high-PIP injury. Recently, Caironi et al. (8) demonstrated that high-tidal volume ventilation impaired the vasoconstriction response, increased alveolar epithelial permeability, elevated BALF levels of cysteinyl LTs (LTC_4, LTD_4, and LTE_4), and increased influx of neutrophils into the air spaces. Increases in these LTs were absent in 5-LOX-knockout mice under the same conditions (8). Even though physiological buffer without blood was used in the present study, the LOX inhibitor significantly inhibited lavage LT concentrations and partially attenuated the increase in permeability, possibly an indication of a neutrophil-independent mechanism of injury, such as an altered epithelial fluid clearance (37). However, nonspecific LOX inhibition may be protective as a result of inhibition of the 5-LOX pathway production of cysteinyl LTs and the 12-LOX production of 12-HETE but will also inhibit 15-LOX production of anti-inflammatory lipoxins (6).

PAF, another of the downstream products generated from phospholipids by $cPLA_2$, may contribute to the increases in vascular permeability. PAF-induced edema formation proceeds by two distinct mechanisms, which are mediated by the inositol 1,4,5-trisphosphate receptor or PGE_2, a COX metabolite (10, 14). In the present study, there were no significant differences in K_{fc} or W/D between the ATK group and the COX + LOX + *P*-450 group. Although the combination of the all inhibitors of COX, LOX, and *P*-450 pathways would not inhibit PAF synthesis directly, the COX inhibitor may have reduced the PAF contribution to the increased K_{fc}, such that K_{fc} in the COX + LOX + *P*-450 group was similar to that in the ATK group.

The decreases in vascular resistance indicated the well-known effects of recruitment and distension of microvessels on vascular resistance (30). In the present study, R_t, especially R_v, in the low-PIP control group decreased significantly at the end of the experiments. In the other groups, R_t decreased transiently at 50 min and increased again at the end of the experiment. Mechanical compression of small vessels by edema may have induced the increased R_t in those groups (32).

Mediators such as TX and PAF are well-known vasoconstrictors of the pulmonary artery (10). Because the COX inhibitor ibuprofen can block the vasoconstrictor effects of TX, as well as the vasodilator effects of PGI_2, these opposing effects could cancel one another and result in the lack of a significant difference in R_t between groups with or without ibuprofen.

In conclusion, cPLA$_2$ activation appears to contribute to the rapid increase in lung vascular permeability of VILI in mice through numerous pathways. The high-pressure lung distension used in the present study induced increases in the levels of various downstream products of AA metabolism, which appear to potentiate each other to increase lung vascular permeability.

GRANTS

This study was supported by National Heart, Lung, and Blood Institute Grant P01 HL-66299.

REFERENCES

1. **Alvarez DF, King JA, Weber D, Addison E, Liedtke W, Townsley MI.** Transient receptor potential vanilloid 4-mediated disruption of the alveolar septal barrier: a novel mechanism of acute lung injury. *Circ Res* 99: 988–995, 2006.
2. **Alvarez DF, Gjerde EA, Townsley MI.** Role of EETs in regulation of endothelial permeability in rat lung. *Am J Physiol Lung Cell Mol Physiol* 286: L445–L451, 2004.
3. **Andersson O, Nordlund-Moller L, Barnes HJ, Lund J.** Heterologous expression of human uteroglobin/polychlorinated biphenyl-binding protein. Determination of ligand binding parameters and mechanism of phospholipase A_2 inhibition in vitro. *J Biol Chem* 269: 19081–19087, 1994.
4. **Azuma N, Duzgun SA, Ikeda M, Kito H, Akasaka N, Sasajima T, Sumpio BE.** Endothelial cell response to different mechanical forces. *J Vasc Surg* 32: 789–794, 2000.
5. **Bhattacharya J.** Interpreting the lung microvascular filtration coefficient. *Am J Physiol Lung Cell Mol Physiol* 293: L9–L10, 2007.
6. **Bogatcheva NV, Sergeeva MG, Dudek SM, Verin AD.** Arachidonic acid cascade in endothelial pathobiology. *Microvasc Res* 69: 107–127, 2005.
7. **Brower RG, Matthay MA, Morris A, Schoenfeld D, Thompson BT.** Ventilation with lower tidal volumes as compared with traditional tidal volumes for acute lung injury and respiratory distress syndrome. *N Engl J Med* 342: 1301–1308, 2000.
8. **Caironi P, Ichinose F, Liu R, Jones RC, Bloch KD, Zapol WM.** 5-Lipoxygenase deficiency prevents respiratory failure during ventilator-induced lung injury. *Am J Respir Crit Care Med* 172: 334–343, 2005.
9. **Curry FE.** Mechanics and thermodynamics of transcapillary exchange. In: *Handbook of Physiology. The Cardiovascular System. Microcirculation*. Bethesda, MD: Am. Physiol. Soc., 1984, sect. 2, vol. IV, pt. 1, chapt. 8, p. 309–374.
10. **Falk S, Goggel R, Heydasch U, Brasch F, Muller KM, Wendel A, Uhlig S.** Quinolines attenuate PAF-induced pulmonary pressor responses and edema formation. *Am J Respir Crit Care Med* 160: 1734–1742, 1999.
11. **Frank JA, Matthay MA.** Leukotrienes in acute lung injury: a potential therapeutic target? *Am J Respir Crit Care Med* 172: 261–262, 2005.
12. **Gama de Abreau M, Wilmink B, Hubler M, Koch T.** Vaporized perfluorohexane attenuates ventilator-induced lung injury in isolated, perfused rabbit lungs. *Anesthesiology* 102: 597–605, 2005.
13. **Goggel R, Hoffman S, Nusing R, Narumiya S, Uhlig S.** Platelet-activating factor-induced pulmonary edema is partly mediated by prostaglandin E_2, E-prostanoid 3-receptors, and potassium channels. *Am J Respir Crit Care Med* 166: 657–662, 2001.
14. **Goggel R, Uhlig S.** The inositol trisphosphate pathway mediates platelet-activating factor-induced pulmonary oedema. *Eur Respir J* 25: 849–857, 2005.
15. **Hamanaka K, Jian MY, Weber DS, Alvarez DF, Townsley MI, Al Mehdi AB, King JA, Liedtke W, Parker JC.** TRPV4 initiates the acute calcium-dependent permeability increase during ventilator-induced lung injury in isolated mouse lungs. *Am J Physiol Lung Cell Mol Physiol* 293: L923–L932, 2007.
16. **Hino Si Tanji C, Nakayama KI, Kikuchi A.** Phosphorylation of β-catenin by cyclic AMP-dependent protein kinase stabilizes β-catenin through inhibition of its ubiquitination. *Mol Cell Biol* 25: 9063–9072, 2005.
17. **Hybertson BM, Bursten SL, Leff JA, Lee YM, Jepson EK, Dewitt CR, Zagorski J, Cho HG, Repine JE.** Lisofylline prevents leak, but not neutrophil accumulation, in lungs of rats given IL-1 intratracheally. *J Appl Physiol* 82: 226–232, 1997.
18. **Kennedy BP, Payette P, Mudgett J, Vadas P, Pruzanski W, Kwan M, Tang C, Rancourt DE, Cromlish WA.** A natural disruption of the secretory group II phospholipase A_2 gene in inbred mouse strains. *J Biol Chem* 270: 22378–22385, 1995.
19. **Kuebler WM, Kuhnle GE, Goetz AE.** Leukocyte margination in alveolar capillaries: interrelationship with functional capillary geometry and microhemodynamics. *J Vasc Res* 36: 282–288, 1999.
20. **Leslie CC.** Properties and regulation of cytosolic phospholipase A_2. *J Biol Chem* 272: 16709–16712, 1997.
21. **Matthay MA, Eschenbacher WL, Goetzl EJ.** Elevated concentrations of leukotriene D_4 in pulmonary edema fluid of patients with the adult respiratory distress syndrome. *J Clin Immunol* 4: 479–483, 1984.
22. **McLean PG, Aston D, Sarkar D, Ahluwalia A.** Protease-activated receptor-2 activation causes EDHF-like coronary vasodilation: selective preservation in ischemia/reperfusion injury: involvement of lipoxygenase products, VR1 receptors, and C-fibers. *Circ Res* 90: 465–472, 2002.
23. **Murakami M, Kudo I.** Phospholipase A_2. *J Biochem (Tokyo)* 131: 285–292, 2002.
24. **Nagase T, Uozumi N, Aoki-Nagase T, Terawaki K, Ishii S, Tomita T, Yamamoto H, Hashizume K, Ouchi Y, Shimizu T.** A potent inhibitor of cytosolic phospholipase A_2, arachidonyl trifluoromethyl ketone, attenuates LPS-induced lung injury in mice. *Am J Physiol Lung Cell Mol Physiol* 284: L720–L726, 2003.
25. **Nagase T, Uozumi N, Ishii S, Kume K, Izumi T, Ouchi Y, Shimizu T.** Acute lung injury by sepsis and acid aspiration: a key role for cytosolic phospholipase A_2. *Nat Immunol* 1: 42–46, 2000.
26. **Nakos G, Kitsiouli E, Hatzidaki E, Koulouras V, Touqui L, Lekka ME.** Phospholipases A_2 and platelet-activating factor acetylhydrolase in patients with acute respiratory distress syndrome. *Crit Care Med* 33: 772–779, 2005.
27. **Naruse K, Sokabe M.** Involvement of stretch-activated ion channels in Ca^{2+} mobilization to mechanical stretch in endothelial cells. *Am J Physiol Cell Physiol* 264: C1037–C1044, 1993.
28. **Nilius B, Droogmans G.** Ion channels and their functional role in vascular endothelium. *Physiol Rev* 81: 1415–1459, 2001.
29. **Park GY, Christman JW.** Involvement of cyclooxygenase-2 and prostaglandins in the molecular pathogenesis of inflammatory lung diseases. *Am J Physiol Lung Cell Mol Physiol* 290: L797–L805, 2006.
30. **Parker JC, Gillespie MN, Taylor AE, Martin SL.** Capillary filtration coefficient, vascular resistance, and compliance in isolated mouse lungs. *J Appl Physiol* 87: 1421–1427, 1999.
31. **Parker JC, Ivey C, Tucker A.** Gadolinium prevents high airway pressure-induced permeability increases in isolated rat lungs. *J Appl Physiol* 84: 1113–1118, 1998.
32. **Parker JC, Ivey CL, Tucker A.** Phosphotyrosine phosphatase and tyrosine inhibition modulate airway pressure-induced lung injury. *J Appl Physiol* 85: 1753–1761, 1998.
33. **Parker JC, Townsley MI.** Evaluation of lung injury in rats and mice. *Am J Physiol Lung Cell Mol Physiol* 286: L231–L246, 2004.
34. **Parker JC, Yoshikawa S.** Vascular segmental permeabilities at high peak inflation pressure in isolated rat lungs. *Am J Physiol Lung Cell Mol Physiol* 283: L1203–L1209, 2002.
35. **Pearce MJ, McIntyre TM, Prescott SM, Zimmerman GA, Whatley RE.** Shear stress activates cytosolic phospholipase A_2 (cPLA$_2$) and MAP kinase in human endothelial cells. *Biochem Biophys Res Commun* 218: 500–504, 1996.
36. **Ricard JD, Dreyfuss D, Saumon G.** Production of inflammatory cytokines in ventilator-induced lung injury: a reappraisal. *Am J Respir Crit Care Med* 163: 1176–1180, 2001.
37. **Sloniewsky DE, Ridge KM, Adir Y, Fries FP, Briva A, Sznajder JI, Sporn PH.** Leukotriene D_4 activates alveolar epithelial Na,K-ATPase and increases alveolar fluid clearance. *Am J Respir Crit Care Med* 169: 407–412, 2004.
38. **Strotmann R, Harteneck C, Nunnenmacher K, Schultz G, Plant TD.** OTRPC4, a nonselective cation channel that confers sensitivity to extracellular osmolarity. *Nat Cell Biol* 2: 695–702, 2000.

39. **Tankersley CG, Rabold R, Mitzner W.** Differential lung mechanics are genetically determined in inbred murine strains. *J Appl Physiol* 86: 1764–1769, 1999.
40. **Taylor AE, Parker JC.** The interstitial spaces and lymph flow. In: *Handbook of Physiology. The Respiratory System. Circulation and Nonrespiratory Function.* Bethesda, MD: Am. Physiol. Soc., 1985, sect. 3, vol. I, chapt. 4, p. 167–320.
41. **Von Bethmann AN, Brasch F, Nusing R, Vogt K, Volk HD, Muller KM, Wendel A, Uhlig S.** Hyperventilation induces release of cytokines from perfused mouse lung. *Am J Respir Crit Care Med* 157: 263–272, 1998.
42. **Wang MH, Brand-Schieber E, Zand BA, Nguyen X, Falck JR, Balu N, Schwartzman ML.** Cytochrome *P*-450-derived arachidonic acid metabolism in the rat kidney: characterization of selective inhibitors. *J Pharmacol Exp Ther* 284: 966–973, 1998.
43. **Watanabe H.** Activation of TRPV4 channels (hVRL-2/mTRP12) by phorbol derivatives. *J Biol Chem* 277: 13569–13577, 2002.
44. **Watanabe H, Vriens J, Prenen J, Droogmans G, Voets T, Nilius B.** Anandamide and arachidonic acid use epoxyeicosatrienoic acids to activate TRPV4 channels. *Nature* 424: 434–438, 2003.
45. **Yoshikawa S, King JA, Lausch RN, Penton AM, Eyal FG, Parker JC.** Acute ventilator-induced vascular permeability and cytokine responses in isolated and in situ mouse lungs. *J Appl Physiol* 97: 2190–2199, 2004.
46. **Yoshikawa S, Miyahara T, Reynolds SD, Stripp BR, Anghelescu M, Eyal FG, Parker JC.** Clara cell secretory protein and phospholipase A$_2$ activity modulate acute ventilator-induced lung injury in mice. *J Appl Physiol* 98: 1264–1271, 2005.
47. **Zhu X, Sano H, Kim KP, Sano A, Boetticher E, Munoz NM, Cho W, Leff AR.** Role of mitogen-activated protein kinase-mediated cytosolic phospholipase A$_2$ activation in arachidonic acid metabolism in human eosinophils. *J Immunol* 167: 461–468, 2001.